FTPG: A Fine-Grained Traffic Prediction Method With Graph Attention Network Using Big Trace Data

Mengyuan Fang, *Graduate Student Member, IEEE*, Luliang Tang, Xue Yang, Yang Chen, Chaokui Li, and Qingquan Li

***Abstract*— Short-term traffic prediction is of great importance to the management of traffic congestion, a pervasive and difficult-to-solve problem in many metropolises all over the world. However, existing studies on traffic prediction contain rough traffic information at the carriageway level that ignore the distinction between different turns in one intersection. With the aim of predicting traffic at road intersections from big trace data on a finer scale, this study proposes a novel method, the fine-grained traffic prediction method (FTPG) with a graph attention network (GAT), which predicts traffic information, including traffic flow speeds, traffic states, and average queue lengths, at the turn level. In the FTPG, a method for estimation of the queue starting point is proposed to improve the accuracy of traffic information detection. Furthermore, the topology is constructed under turn-level conditions, and a GAT-based method, the spatio-temporal residual graph attention network (ST-RGAN), is proposed to improve the prediction accuracy. Experiments are performed using taxi GPS trace data collected in the city of Wuhan and show that the proposed FTPG method can make predictions with fine-grained traffic information for road intersections accurately and robustly.**

***Index Terms*— Short-term traffic prediction, big data, graph neural network, road intersection, turn level.**

I. Introduction

With the rapid development of urbanization and fast economic growth, city residents' travel demands have a steep growth trajectory that contradicts the limited traffic capacity [1]. As a result, urban traffic congestion tends to be severe and is not only costly in terms of time and economic activity [2]–[4] but also the cause of increased transportation noise and air pollution [5], [6]. To reduce the impact of traffic congestion in urban areas, accurate short-term traffic predictions have become a hot research topic [7]. The effective and prospective traffic information both supports the ability to create effective strategies for optimizing traffic assignments and provides references for travellers to plan the time-dependent optimal path [4], [8], [9]. Therefore, traffic information acquisition and short-term prediction have become a research hotspot in the field of intelligent transportation.

Compared with measurement approaches using fixed sensors, detecting traffic information using floating-car trace data is a better solution with a wider range and lower cost. With the development of ride-hailing and intelligent transportation systems, it is easy to collect real-time vehicle trace data on the road, and the traffic detection based on floating-car trace data are widely used. [2], [10]–[17] proposed methods to obtain traffic information parameters, such as the traffic state, queue length, and travel time, by using floating-car trace data. [8], [11], [18]–[25] further proposed methods of short-term traffic prediction.

Road intersections, as the link point of the road network, are the areas where the probability of traffic congestion is relatively high and should attract research attention [1], [14], [26]. Further, as the traffic inside intersections is usually complicated, fine-grained traffic predictions for road intersections are of great significance [2], [12], [14]. However, most of the present studies on intersection traffic prediction with trace data provide rough information (e.g., traffic state and traffic speed) at the regional level or carriageway level. When the difference between lanes and directions within intersections is not distinguished, the reliability and accuracy of further application is affected, such as travel time estimation and traffic dispersion [11], [12], [14].

To achieve finer-grained traffic information prediction, this research proposes a fine-grained traffic prediction method based on the graph attention network (FTPG) from big trace data, which can predict traffic information at the turn level. The FTPG method includes two parts, namely, fine-grained traffic information detection and short-term traffic prediction. A novel estimation method is proposed in the former part to improve the accuracy of traffic information detection using low-frequency trace data, and a graph-based method

Manuscript received July 9, 2020; revised November 1, 2020; accepted December 17, 2020. This work was supported in part by the National Key Research and Development Plan of China under Grant 2017YFB0503604 and Grant 2016YFE0200400 and in part by the National Natural Science Foundation of China under Grant 41971405, Grant 41671442, and Grant 41901394. The Associate Editor for this article was J. E. Naranjo. *(Corresponding authors: Luliang Tang; Xue Yang.)*

Mengyuan Fang, Luliang Tang, and Yang Chen are with the State Key Laboratory for Information Engineering in Surveying, Mapping, and Remote Sensing, Wuhan University, Wuhan 430072, China (e-mail: tll@whu.edu.cn).

Xue Yang is with the School of Geography and Information Engineering, China University of Geosciences, Wuhan 430074, China (e-mail: yangxue@cug.edu.cn).

Chaokui Li is with the National-Local Joint Engineering Laboratory of Geo-Spatial Information Technology, Hunan University of Science and Technology, Xiangtan 411201, China.

Qingquan Li is with the Key Laboratory for Geo-Environment Monitoring of Coastal Zone of the National Administration of Surveying, Mapping, and GeoInformation, Shenzhen University, Shenzhen 518060, China.

Digital Object Identifier 10.1109/TITS.2021.3049264

is proposed in the latter part to achieve a more accurate prediction.

Importantly, the emphasis on "fine-grained" in FTPG is embodied in two aspects. From the aspect of spatial granularity, the provided traffic information of FTPG is at turn-level scale, which is more elaborate than that at regional-level or carriageway-level scale. From the aspect of the information dimension, the predictive information of FTPG includes the traffic state, traffic flow speed, and average queue length, which is more abundant than that in existing studies.

The major contributions of this research are summarized as follows.

1) The traffic information (e.g., traffic flow speed, traffic state, and average queue length) has been detected and predicted at the turn level using trace data that can be applied to a wide range of scenarios with low cost.

2) A novel estimation of the queue starting point method is proposed to improve the accuracy of traffic information detection using low-frequency trace data.

3) The graph of the road network is constructed at the turn level, and a traffic prediction model is proposed based on GAT, which has higher accuracy than the benchmark methods.

The remainder of this paper is organized as follows: Section 2 summarizes related works on intersection traffic prediction. Section 3 introduces the key aspects of the FTPG. Section 4 evaluates the proposed FTPG method. Finally, Section 5 concludes this work.

II. Related Work

This section gives an overview of the related works in intersection traffic prediction, including the two aspects of intersection traffic detection and short-term traffic predictions.

A. Intersection Traffic Information Detection

Historical and current traffic information is the premise of traffic prediction, and the traffic information is usually described by parameters such as traffic flow speed, traffic volume, and travel time.

Existing methods of obtaining traffic information can be classified into two categories: methods based on fixed sensors and methods based on floating-car data. Fixed sensors, including licence plate recognition (LPR) cameras [21], [27], loop detectors [28], and Bluetooth detectors [29], measure the traffic flow speed and volume by physical or image processing methods. However, due to the fixed location of sensors and the expensive cost of sensor construction and maintenance, the wider-range application of sensors in monitoring urban traffic is limited. Conversely, as an approach for mobile crowd sensing, the methods based on floating-cars can provide nearly an entire traffic state view for an urban road network with a lower establishment cost [11]–[13], [30]

Traffic detection with floating-car data comprises two categories of methods, namely, the methods based on vehicle-to-everything (V2X) communications data [31] and those based on trace data. At present, the former is limited by communication distances and the penetration rate of the V2X equipment, so it is also difficult to implement on a large scale. The development of ride-hailing and intelligent transportation systems makes it easier to collect real-time vehicle trace data on the road, and the methods based on floating-car trace data are widely used [6], [16], [17], [30].

To obtain the traffic flow information for intersections, [10], [11], [15], [32], [33] put forward methods to estimate the travel time, time delays, queue lengths, and traffic flow speeds of intersections using floating-car trace data. [2], [11], [12] more subtly identified traffic flows in the intersections with different turns, obtaining turn-level traffic information. However, these approaches still have limitations. 1) The accuracy of traffic information depends on the density and sampling frequency of the trace data. 2) Most of the methods require comprehensive and detailed system modelling based on prior knowledge, rendering them unable to accurately describe the variations in traffic data in complex real-world environments [11]. 3) The current position accuracy of floating-car traces is a metre-level value that limits further lane-level traffic information [2].

B. Short-Term Traffic Prediction

Short-term traffic prediction is one of the important capabilities in the field of intelligent transportation systems (ITSs) [12], [19], [34]. Since the road traffic in the traffic network is in a process of spatio-temporal dynamic evolution, the core aspect of short-term traffic prediction is the ability to model the spatio-temporal patterns of traffic networks [24], [25], [35].

Early research was mainly based on model-driven methods, such as the autoregressive integrated moving average (ARIMA) [36], Kalman filter [37], and Bayesian network [11], [20], [21]. Given the dependence on the assumption of stationarity, these methods failed to handle complex traffic scenarios. During the last decade, new attempts to predict traffic information have used data-driven approaches, such as, support vector regression (SVR) models [38], long short-term memory (LSTM) networks [39], and deep belief networks (DBNs) [18]. However, these methods lack consideration of spatial characteristics [19], [22].

To introduce spatial patterns to road traffic, [9], [35], [40] divided continuous space into grids and adopted an image-based method, convolutional neural networks (CNNs). Though these studies achieved a higher prediction accuracy, there are still limitations in expressing the geometry and topological relationships of road traffic using regular grids [23], [25]. As a better solution, constructing the road topology with a graph and adopting the graph neural network (GNN) models, such as the graph convolution network (GCN), can further improve the accuracy of prediction [25], [41]. Recently, researchers have made efforts to introduce an attention mechanism into GNNs aiming at capturing more complex spatial patterns of the data [24].

These above studies have proposed superior methods for short-term traffic prediction; nevertheless, most of them were focused on arterial highways with carriageway-level considerations and lacked consideration of the traffic information in urban intersections.

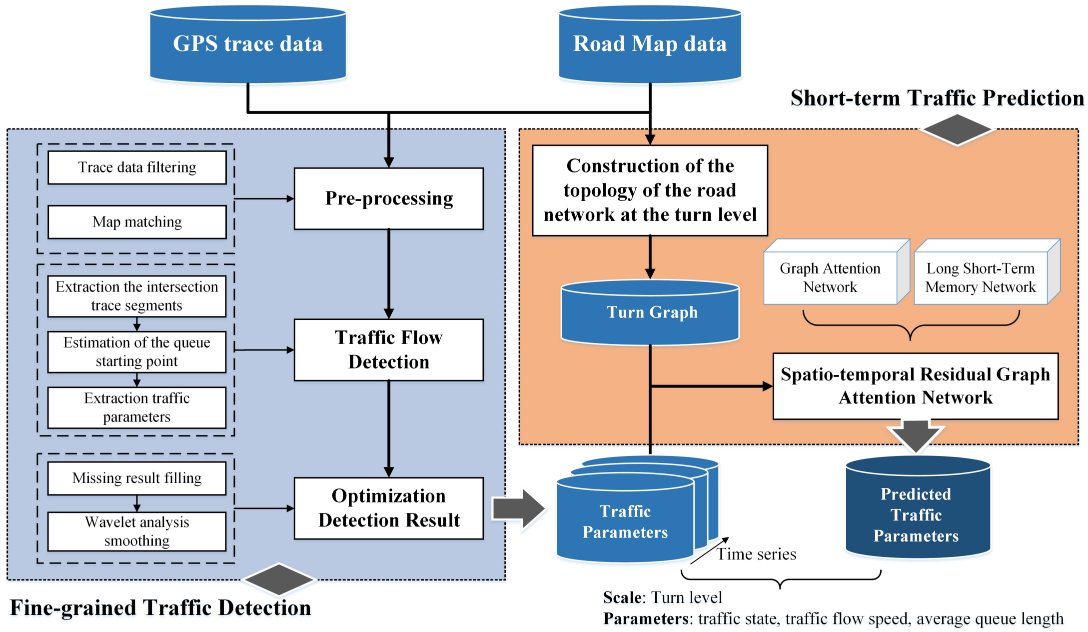

Fig. 1. Architecture of the FTPG method.

TABLE I
RELATED STUDIES ON INTERSECTION TRAFFIC PREDICTION

Related works	Data acquisition	Implementation range	Differentiation of turns	Predictive content
[1]	Traffic sensors	Wide	No	Traffic volume
[18]				
[42]				Traffic state
[43]	Licence plate recognition camera	Local	Yes	Queue length
[44]		Local		
[21]		Local		Queue length & traffic state
[11]	Floating-cars	Wide		Travel time

With the adoption of the above methods, several related works have focused on traffic predictions of urban intersections, which are summarized in Table I.

According to Table I, the following limitations can be summarized. 1) Most of these studies predict just one kind of traffic information. 2) Although some studies can differentiate lanes or turns with LPR cameras, as described in Section II.A, the cost of equipment installation and maintenance limits their wider range of application. 3) Although [11] has achieved a wide range of refined prediction of travel time in intersections with flow modelling and machine learning, the accuracy is still limited by the traffic flow assumptions and sampling frequency of GPS data.

Based on the above review, it was desirable to develop a fine-grained, low-cost, reliable traffic prediction method. Therefore, the objective of this research is to extend previous studies in the following ways: 1) Enhance the refinement of traffic states by distinguishing the difference between turns and increasing the information richness; 2) improve the accuracy of traffic detection from big trace data without additional information; 3) improve the accuracy of traffic prediction by modelling the spatio-temporal patterns.

III. METHODOLOGY

Aiming to achieve a finer-grained traffic information prediction, this research proposes a fine-grained traffic prediction method based on the graph attention network (FTPG) from big trace data, which can predict the traffic information at the turn level. The architecture of the FTPG method is shown in Fig. 1. The FTPG method is composed of two parts:

Part 1: Fine-grained Traffic Detection. This part detects traffic information for road intersections at turn-level conditions including the traffic flow speed, traffic state, and average queue length, using low-sampling GPS trace data.

Part 2: Short-term Traffic Prediction. To improve the accuracy by effectively modelling the spatial dependency, this part constructs the graph structure of the road network at the turn level and adopts a proposed GAT-based deep learning model to predict future traffic information.

As a data-driven method, in the training stage, the historical trace data are processed with Part 1 all at once as the training dataset of Part 2; in the testing stage, the real-time trace data are processed with Part 1, and then the current and historical results of Part 1 are jointly entered into Part 2 to predict the future traffic parameters.

A. Fine-Grained Traffic Detection

The current and historical traffic information is a pre-condition of short-term traffic prediction [35], [41]. Due to the limitations in positioning and communication capabilities, the sampling interval of floating-car trace data is usually within a range of 20-60 s. Therefore, with the goal of detecting the traffic information at the turn level using low-frequency (20-60 s) trace data, the process includes three steps: pre-processing, traffic flow detection, and optimization detection results.

Referring to earlier works by [45] and [46], the pre-processing step tries to match the trace point with its roads and filter out the points with gross errors.

Details of the traffic flow detection and optimization detection result processes are presented in the following sub-sections.

1) Traffic Flow Detection:

a) Extraction of intersection trace segments: To obtain road intersection traffic information, the first step is to extract the trace points from within the intersections. It is well known that a floating car slows down and starts to queue while entering the intersection. Therefore, the trace is split at the sample point where a car begins to slow down near an intersection, and the continuous trace sample points are reserved from the point of slowing down to the point of driving away from the intersection as intersection trace segments [2].

b) Estimation of the queue starting point: In the existing studies, the queue starting point is represented by the trace sample point, for instance, the point before slowing down $P_s(x_s, y_s, t_s, v_s)$ or the point after slowing down $P_e(x_e, y_e, t_e, v_e)$. However, there is a gap between the above two points, and the adoption of the above two points will bring uncertainty to the queue average extraction.

The gap depends on the trace sampling interval. Taking a vehicle driving at an average of 10 km/h as an example, the gap is not less than 56 metres under the sampling interval of 20s. Associated with the gap, the actual queue starting point is uncertain. Therefore, a novel queue starting point estimation method is proposed to improve the accuracy affected by this uncertainty.

When a vehicle enters an intersection, the deceleration of the vehicle ranges from $2.2m/s^2$ to $5.9m/s^2$ [47]. For example, the deceleration distance is approximately 5-14 metres and the time interval is approximately 1-2.68 s when a vehicle enters an intersection with a speed of 30 km/h and slows down to 10 km/s. Compared with the sampling interval of 20-60 s, the deceleration process can be regarded as a tiny process contained within P_s and P_e. In this research, the tiny process is simplified as a breakpoint with a speed change. Semantically, that breakpoint is the queue starting point of the vehicle. Theoretically, the uncertainty is reduced from 56 to less than 14 metres.

While precise determination of the process of driving involved in the trace sampling points is not possible, in this research, the process is categorized as two patterns to estimate the queue starting point, according to the instantaneous speed and the mean speed between the two points:

For Pattern 1, because the v_m is between two instantaneous speeds, the speed of the vehicle is approximately monotonically decreasing. Then, the driving process can be simplified as a "uniform speed travel - slow down - uniform speed queue" process, as shown in Fig. 3(a). According to $s = \int v dt$, the queue starting point (x', y', t') can be calculated as (1):

$$
\begin{aligned}
d &= \sqrt{(x_e - x_s)^2 + (y_e - y_s)^2} \\
t' &= t_s + \frac{d - v_e(t_e - t_s)}{v_s - v_e}
\end{aligned}
$$

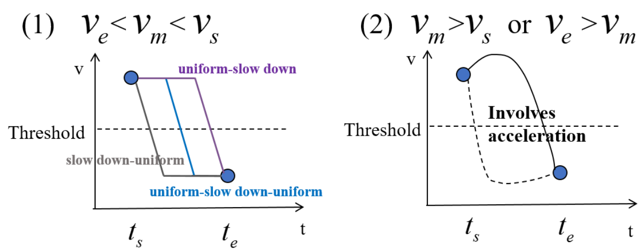

Fig. 2. Two patterns of speed change in an intersection.

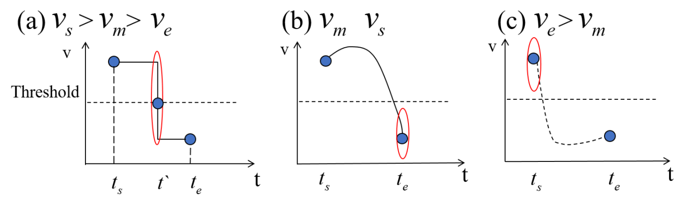

Fig. 3. Estimation of the queue starting point for two patterns.

$$
\begin{aligned}
x' &= x_s + \frac{x_e - x_s}{s} v_s (t' - t_s) \\
y' &= y_s + \frac{y_e - y_s}{s} v_s (t' - t_s)
\end{aligned} \tag{1}
$$

For Pattern 2, if the mean speed v_m is higher than v_s or lower than v_e, there must be an acceleration process. Since the process of motion cannot be estimated, the queue starting point is approximated: if 1_m is higher than v_s, the vehicle experienced a "speed up - slow down" process, namely, the queue starting point is closer to P_e, and thus, P_e is approximated as the queue starting point, as shown in Fig. 3(b); correspondingly, P_s is approximated as the queue staring point when v_m is lower than v_e, as shown in Fig. 3(c).

c) Extraction of traffic parameters: With the estimation above, a more precise trace segment collection of intersections is obtained. According to the direction angle of the car entering and leaving the intersection, the trace segments can be matched with their turns. Then, the traffic parameters of each turn can be extracted.

As the most commonly used parameters, traffic flow speed and traffic volume were used to evaluate the traffic state [3], and the queue length can reflect the time delay of passing through the intersection [33], [48]. Since the real-time proportion is unknown, it is not possible to obtain traffic volume using trace data.

Traffic parameters fluctuate dramatically under the influence of traffic lights. As we are interested in the traffic trends more than in fluctuations, to obtain the trends, the results are aggregated within an aggregation interval that is typically on the order of 5-15 minutes [37].

In this research, the traffic parameters are defined as follows.

Definition 1 (Traffic Flow Speed): The mean speed is the average of a vehicle's speed from entering an intersection to leaving it. Furthermore, the traffic flow speed is the average of the mean speed of vehicles within the aggregation interval.

$$
V_{t,k} = \frac{\sum_{i=1}^{n} \frac{dis(P^i_{t,k}, P^i_l)}{t^i - t^i_l}}{n} \tag{2}
$$

Definition 2 (Average Queue Length): The queue length denotes the length of the queue of the vehicle stuck in congestion at an intersection or waiting at the signal [2]. Furthermore, the average queue length is the average value of the queue length within the aggregation interval:

$$AQL_{t,k} = \frac{\sum_{i=1}^{n} dis(P_{t,k}^{i}, P_j)}{n} - R_j \tag{3}$$

Definition 3 (Traffic State): Referring to [2], the grade of the traffic performance can be divided into four states, namely, serious congestion, medium congestion, slight congestion, and smooth with the free-flow speed. The free-flow speed can be obtained by picking the speed value of a turn at the 85% position speed; then, the current traffic state is transformed from the current traffic flow speed, compared with the free-flow speed:

$$\begin{aligned} &State_{t,k} \\ &= \begin{cases} SeriousCongestion & V_{t,k} < 0.47V_k^{free} \\ MediumCongestion & 0.47V_k^{free} < V_{t,k} < 0.56V_k^{free} \\ SlightCongestion & 0.56V_k^{free} < V_{t,k} < 0.66V_k^{free} \\ Free & 0.66V_k^{free} < V_{t,k} \end{cases} \end{aligned} \tag{4}$$

In (2-4), t, k, and j are the tth aggregation interval, kth turn, and jth intersection, respectively; n is the count of the trace segments of the tth aggregation interval and kth turn; $P_{t,k}^{i}$ and P_l^i are the queue start point and last point of the ith trace segments, respectively; t^i and t_l^i are the time of the queue start point and last point of the ith trace segments, respectively; and P_j, R_j are the centre point and radius of the jth intersection, respectively. V_k^{free} is the free-flow speed of the kth turn.

2) *Optimization Detection Result:* The density of the floating-car trace affects the quality of the detection results [11], [32], namely, the uneven distribution of sparse data results in an unstable result, especially during night-time or across signal cycles.

Since the traffic information data have continuity and periodicity in the time dimension [17], [25], to obtain results closer to the real traffic situation, the results can be optimized with historical results, and the data curves with high-frequency leaps can be smoothed by wavelet analysis.

a) Missing result filling: According to the correlation and periodicity in the temporal dimension, missing results are filled with the results of previous aggregation intervals and the same interval of previous days, as in (5). The weight depends on the correlation between the historical moment and the target moment, that is, the stronger the correlation is, the closer the time series are. As in (6) and (7), the Pearson correlation coefficient is adopted to calculate the weight.

$$x = \frac{\sum_{i=1}^{n} W_i^r x_i^r + \sum_{j=1}^{m} W_j^d x_j^d}{\sum_{i=1}^{n} W_i^r + \sum_{j=1}^{m} W_j^d} \tag{5}$$

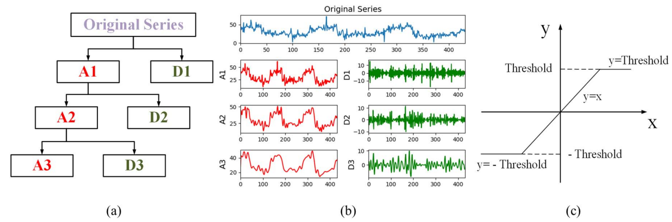

Fig. 4. Wavelet decomposition and filtering: (a) Wavelet decomposition, (b) example of wavelet decomposition result, (c) filter function.

$$\begin{aligned} W_i^r &= \rho(X_{c-T}^{c}, X_{c-i-T}^{c-i}) \\ &= \frac{Cov(X_{c-T}^{c}, X_{c-i-T}^{c-i})}{\sqrt{Var[X_{c-T}^{c}] \cdot Var[X_{c-i-T}^{c-i}]}} \end{aligned} \tag{6}$$

$$\begin{aligned} W_j^d &= \rho(X_{c-T}^{c}, X_{c-(j+1)\cdot T}^{c-j\cdot T}) \\ &= \frac{Cov(X_{c-T}^{c}, X_{c-(j+1)\cdot T}^{c-j\cdot T})}{\sqrt{Var[X_{c-T}^{c}] \cdot Var[X_{c-(j+1)\cdot T}^{c-j\cdot T}]}} \end{aligned} \tag{7}$$

where n and m represent the count of the previous aggregation interval's data and the previous day's data, respectively;x_i^r and x_j^d represent the ith and jth previous interval's data and previous day's data, respectively; ρ represents the correlation coefficient of two groups of variables; X_p^q represents the group of previous data from interval p to q; c represents the current interval and T represents the count of intervals per day.

b) Wavelet analysis smoothing: As mentioned above, the evolution of traffic occurs as a continuous trend, which can be regarded as a low-frequency, continuous signal. However, due to the influence of sparse data or the cycle signals, the detection result series contain noise, which presents as a high-frequency signal causing leaps of the curve.

To reduce the noise, the detection results are smoothed by wavelet analysis. As Fig. 4 shows, first, the traffic parameter's time series is decomposed with a wavelet analysis, resulting in the low-frequency signals A1, A2, A3…and the high-frequency signals D1, D2, D3….Then, the high-frequency signals are filtered with a threshold. If the signal strength is higher or lower than the threshold, it is set to the threshold. Finally, the low-frequency signals are fused with the filtered high-frequency signals. As a result, the final signal is smooth without tremendous leaps. The selection of the threshold depends on the changing trend of the data itself.

B. Short-Term Traffic Prediction

Future traffic information parameters can be predicted with the historical time series of traffic information and the proposed deep learning method. Due to the spread of traffic congestion across the road network, there is a correlation between upstream and downstream intersections, forming the traffic spatial dependency [25], [41], which contributes to the accuracy of the prediction [35]. The road network is presented as a graph, and then the GNN method can effectively learn the spatial dependency within the graph [24]. Therefore, in this research, a novel GNN-based method is proposed to achieve accurate prediction.

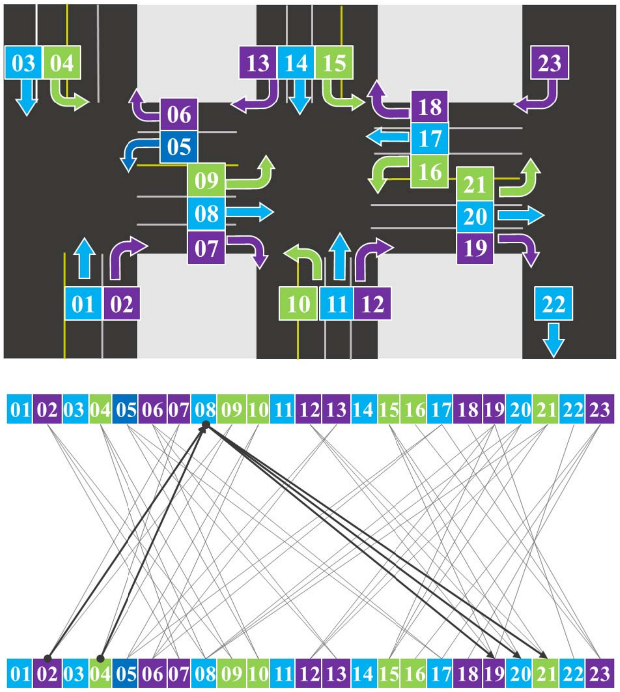

Fig. 5. Schematic diagram of the construction of a turn graph.

1) Topology of the Road Network at the Turn Level: The graph is usually used to represent the topological structures or relational networks as the input of the graph-based model. In the graph, $G = (V, E)$, V is the set of nodes, and E is the set of edges. Though the road network is naturally represented by the graph in which the intersections are regarded as nodes and the roads are edges, it lacks the expression of the turns within the intersections. Dual graph theory [49] is usually used to introduce the link of the road, namely, the turn, with the road network. Nevertheless, in this research, the connectedness of turns needs to be further introduced to represent the correlation of the connecting turn. As a result, the dual graph is applied twice to construct the topology of turns which is called the turn graph in this paper.

In the turn graph, turns in the road network are regarded as the nodes and the turns are linked as edges according to a 1-order connectedness between the upstream and downstream intersections.

As shown in Fig. 5, for example, the #8 turn is connected with the #2 and #4 turns (in the upstream intersection) and the #19, #20, and #21 turns (in the downstream intersection). Then, there will be edges between the #8 turn and #2, #4, #19, #20, and #21 turns. When all the edges are established, the turn graph is generated, which can express the adjacency relationship of turns in the road network.

2) Spatio-Temporal Residual Graph Attention Network: Fully utilizing the spatial and temporal dependencies is the key to solving traffic prediction problems [25], [41]. The LSTM has been proven to capture temporal variability features effectively [50]. The GNN can learn the spatial dependency of the road topology graph [41]. Therefore, in this research, a novel GNN architecture, GAT [51], is adopted with the LSTM to construct a deep learning model that has the ability to learn the spatio-temporal dependencies simultaneously. The proposed model is named the spatio-temporal residual graph attention network (ST-RGAN).

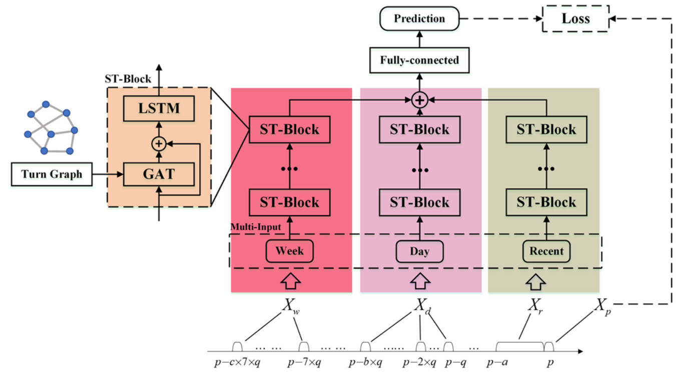

Fig. 6. Architecture of ST-RGAN: a, b, and c represent the number of the input historical data of three branches; q represents the number of intervals during one day.

Fig. 6 presents the architecture of the ST-RGAN model. (1) The ST-RGAN consists of three branches with the same structure and takes historical data for different spans as data input to model the periodicity and continuity of the traffic evolution. (2) The GAT and LSTM are combined as the ST-Block, which is a unit to learn the spatio-temporal pattern. (3) Ultimately, all the three branches are finally fused through the fully connected layer to generate the final prediction results.

a) Multi-branches: With the "workweek-weekend" circulation and the regular daily routines of people, the traffic state shows periodicity on the daily scale and the weekly scale [9]. Though there is existing research [22], [52] that has adopted the GNN or LSTM to build prediction models, these models take only the previous time interval's traffic information parameters into account to model the short-term trend, ignoring the large-scale temporal characteristics of the traffic circulation. Inspired by [9], [24], the proposed ST-RGAN sets three branches, *Week*, *Day*, and *Recent*, taking different spans of historical data as input to model the weekly periodic, daily periodic, and short-term trend respectively.

As Fig. 6 shows, the time series $X_r = \{x_{p-1}, x_{p-2}, \ldots, x_{p-a}\}$, $X_d = \{x_{p-q}, x_{p-2q}, \ldots, x_{p-b\times q}\}$, and $X_w = \{x_{p-7q}, x_{p-14q}, \ldots, x_{p-c\times 7q}\}$ are inputs to the *Recent, Day,* and *Week* branches, respectively. The three inputs consist of the data over the past a intervals of the predicting interval, the data in the past b days at the same time as the predicting interval, and the data in the last c weeks that have the same week attributes and time as the predicting interval.

b) Spatio-temporal block: To capture both spatial and temporal dependencies of the turn graph simultaneously, GAT and LSTM are combined as an ST-Block to jointly process the graph-structured time series. The block itself can be stacked or extended based on the scale and complexity of particular cases. In the ST-Block, a residual connection is formed to GAT, which improves the fitting of the graph-structured feature.

The ST-Block can be formulated as:

$$\begin{aligned} x^{(l+1)} &= \mathrm{F}(x^{(l)}, A) \\ &= \mathrm{ReLU}(\mathrm{LSTM}(x^{(l)} + \mathrm{ReLU}(\mathrm{GAT}(x^{(l)}, A)))) \end{aligned} \quad (8)$$

where $x^{(l)}$ and $x^{(l+1)}$ are the input and the output feature of lth ST-Block, respectively, and A is the adjacency matrix of the turn graph.

GAT is a novel GNN architecture that operates on graph-structured data. Compared with GCN, GAT can effectively improve the learning ability of complex spatial features by learning the weights between adjacent nodes using the self-attention strategy [53].

The LSTM is a variant of recurrent neural networks (RNNs). By introducing the gating units and cell states to control the flow of information, the LSTM solves the vanishing gradient problem and the long-term dependency problem of the general RNNs. The LSTM has been proven to capture temporal variability features effectively and are widely used in time series predictions [22].

For more details of the GAT and LSTM algorithms, please refer to [50], [51].

The superiority of the proposed ST-RGAN can be summarized as follows:

- The three branches can effectively model the long-term trend, periodicity, and short-time trend, which can capture the temporal features coherently.
- GAT can further improve the learning ability of complex spatial features by a self-attention strategy to enhance the accuracy.
- By stacking the multi-layers of the ST-Block, the high-dimensional complex spatio-temporal dependency of traffic can be modelled.

IV. Experiments

The experiments are performed using GPS trace data collected in the real world to analyse the validity and accuracy of the FTPG method.

A. Experimental Setting

1) Dataset: Taxi GPS trace data collected in Wuhan from 1 July 2018 to 18 September 2018 from approximately 4000 taxis are used in the experiments. The sampling time of the trace is within the range of 10-60 s. In the experiment, 31 main plane-intersections with frequent congestion are adopted as research objects. The selected intersections are distributed throughout Wuhan Inner-Ring Road, Jianshe Avenue, and Youyi Avenue, whose distributions are shown in Fig. 7.

2) Settings:

a) Experimental settings: The complete process of the FTPG method is executed with the following settings.

(1) In the traffic flow detection process, the traffic flow speed and average queue length of each turn are detected and aggregated within the time interval of 10 minutes, and then the traffic state is transformed from the traffic flow speed.

(2) In the step of the optimization detection result, the previous 6 periods and previous 7 days' data are used to estimate the missing current traffic parameter data; then, the time series is smoothed with a 3-layer wavelet decomposition by a sym-5 wavelet function.

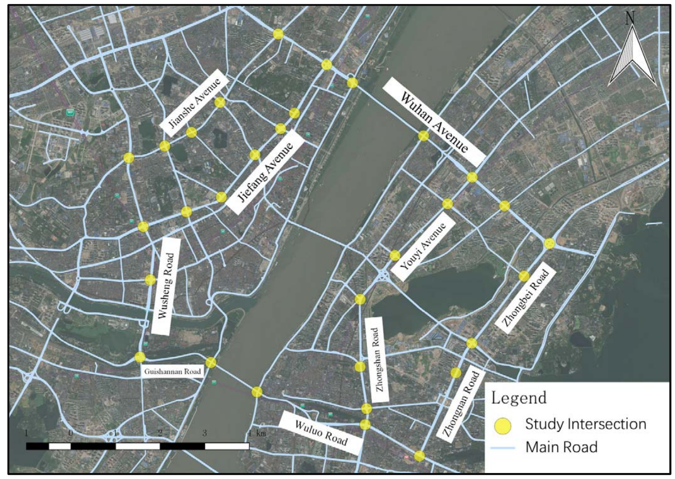

Fig. 7. Selected intersections in the study area.

TABLE II
HYPERPARAMETERS OF ST-RGAN IN THE EXPERIMENT

Layer Name		Recent	Day	Week
Multi-Input		Input Size: N*12	Input Size: N*7	Input Size: N*4
ST-Block-1	GAT	Units: 72 Heads: 7 Activation: *ReLU*	Units: 42 Heads: 7 Activation: *ReLU*	Units: 24 Heads: 7 Activation: *ReLU*
	LSTM	Units: 72 Activation: *Tanh*	Units: 72 Activation: *Tanh*	Units: 72 Activation: *Tanh*
ST-Block-2	GAT	Units: 128 Heads: 7 Activation: *ReLU*	Units: 84 Heads: 7 Activation: *ReLU*	Units: 48 Heads: 7 Activation: *ReLU*
	LSTM	Units: 72 Activation: *Tanh*	Units: 72 Activation: *Tanh*	Units: 72 Activation: *Tanh*
Prediction		Output Size: N*1, Activation: *Tanh*		

(3) The traffic flow speed and average queue length are normalized by the Z-score method as the inputs. The parameters are divided into training and testing sets with proportions of 70% and 30%, respectively.

(4) In the training stage, the ST-RGAN is trained with an Adam optimizer for 100 epochs. The learning rate, batch size, and the loss function are set as $1e^{-3}$, 100, and the mean square error function, respectively.

(5) In the testing stage, to analyse the performance, the ST-RGAN predicts the traffic flow speed and average queue length of the next 10, 20, and 30 minutes and the future 60 minutes in increments of 10 minutes.

b) Hyperparameters of ST-RGAN: Through pre-test and comparison, we set 2-layer ST-Blocks for every branch of ST-RGAN. The hyperparameters of the ST-RGAN are shown in Table II, where the N presents the count of the nodes.

B. Experimental Results

1) Fine-Grained Traffic Detection:

a) Traffic detection result: All the traffic parameters of the road intersections are detected at the turn level with the

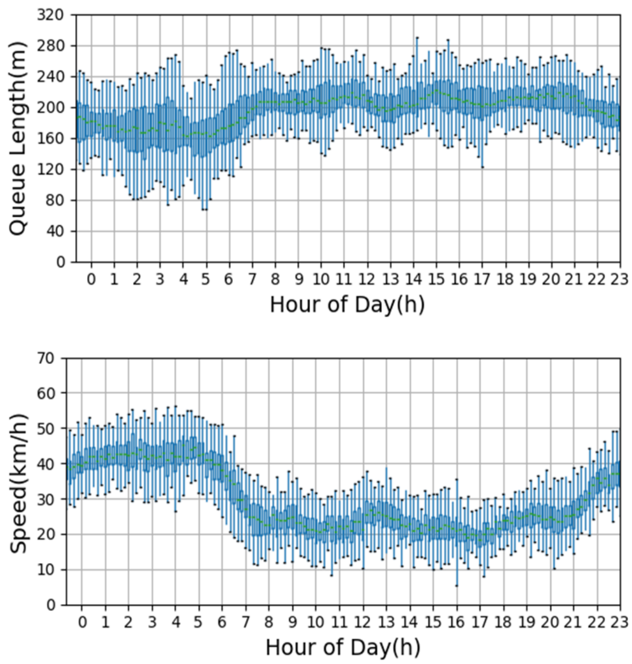

Fig. 8. Average queue length and traffic flow speed of the #20 turn within 70 days.

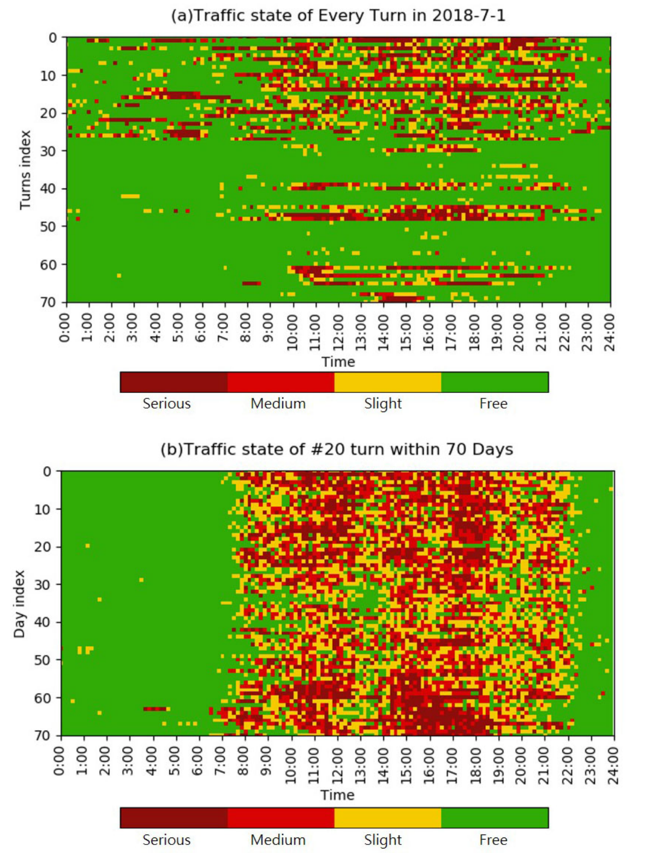

Fig. 9. (a) Traffic state on one day and (b) traffic state of the #20 turn within 70 days.

trace data and the parameters of one turn, and #20 is selected for presentation. The traffic flow speed and average queue length of the #20 turn are presented through the box diagrams in Fig. 8, and the traffic state of all intersections is shown in Fig. 9.

According to the figures, the traffic parameters have a similar pattern between days with a small range of variation at the same time of different days, reflecting the periodicity of the traffic. Moreover, the traffic state varies between the intersection turns, proving that it makes sense to study intersection traffic information under turn-level conditions.

b) Comparison: In the FTPG method, a novel queue starting point estimation method is adopted, and the detection results are optimized with historical data and wavelet analysis. To analyse the superiority of the improved method, the results without the improvements are adopted for comparison, namely, taking the sampling point P_s before the part of slowing-down or the point P_e after the part of slowing-down as the queue starting point to calculate the traffic parameters.

Since there are no ground-truth data available for the traffic information of the experimental area, the autocorrelation coefficient is adopted to indirectly reflect the accuracy. Due to the regular daily routines of people, the traffic data show repeated patterns between days [7], [29], [34], that is, the autocorrelation analysis of the time series can indirectly reflect the accuracy of the detected traffic information, namely, higher accuracy detection results can lead to a higher correlation of its time series.

The autocorrelation coefficient of the detection results is presented in Table III, where QSP represents the queue starting point. The autocorrelation coefficient of our method outperforms the comparison results, confirming that noise is eliminated and the accuracy is effectively enhanced.

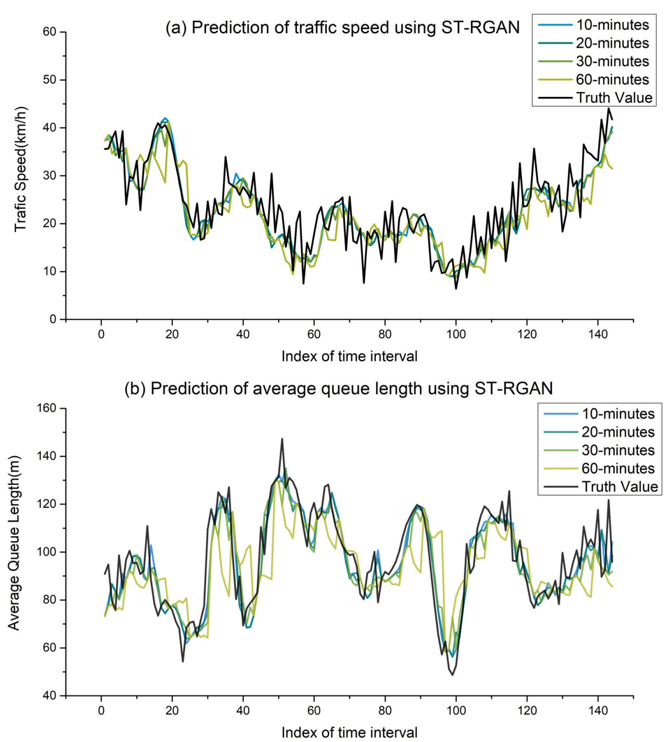

Fig. 10. Visualization of the traffic prediction result.

2) Short-Term Traffic Prediction:

a) Traffic prediction result: To intuitively understand the traffic prediction result of the proposed ST-RGAN, the

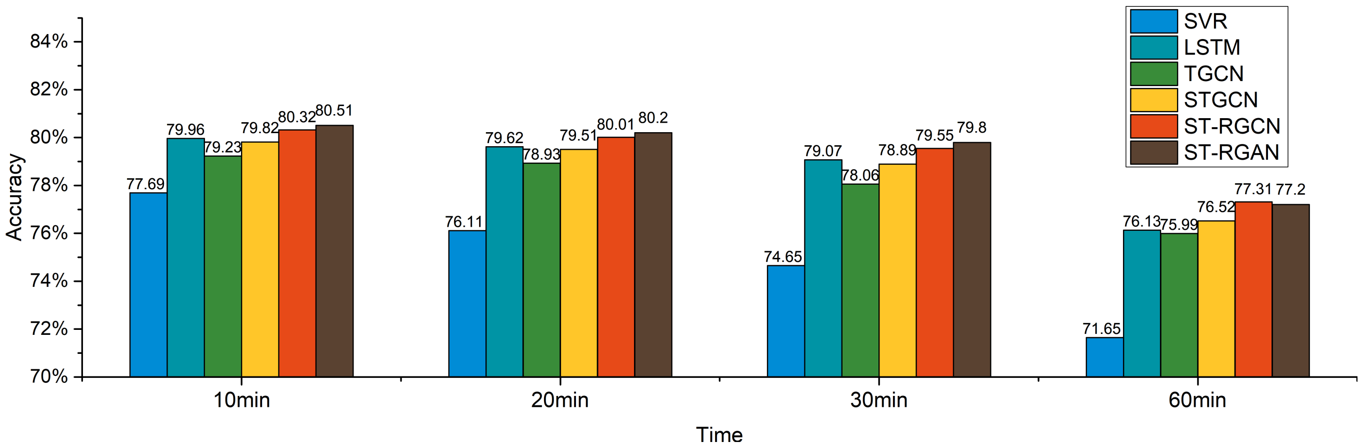

Fig. 11. Scores of different prediction models.

TABLE III
COMPARISON OF THE PEARSON CORRELATION COEFFICIENTS OF THE DETECTION RESULTS

Correlation coefficient	P_s as QSP	P_e as QSP	Our method
Traffic flow speed	0.65	0.63	**0.83**
Average queue length	0.21	0.27	**0.53**

#20 turn is selected for presentation. Fig. 10 shows the visualization prediction results of traffic speed and average queue length in one day, under the time spans of 10, 20, 30 and 60 minutes, together with the traffic detection results as the truth value.

According to the figures, the prediction results are close to the truth value and have the same variation trend, though the frequent fluctuation of the truth value is difficult to fit.

b) Comparison: To evaluate the accuracy and superiority of the ST-RGAN, some of the popular methods of traffic prediction are selected as a baseline for comparison.

(1) SVR: Support vector regression, a popular machine learning regression that has great advantages in non-linear regression.

(2) LSTM: LSTM is a variant of the RNN, which is widely used in time-series prediction.

(3) T-GCN [25]: A deep learning model for traffic prediction based on the GCN and GRU.

(4) ST-GCN [41]: A deep learning model for traffic prediction based on the GCN and CNN.

(5) ST-RGCN: A model that has the same structure as ST-RGAN in which the GAN is replaced with the GCN.

Root mean square error (RMSE) and mean absolute error (MAE), as in (9) and (10), are used as evaluation metrics to evaluate the accuracy of the numerical result. In addition, a metric *score* is defined to evaluate the accuracy of the traffic state, as (11).

$$RMSE = \sqrt{\frac{\sum_{i=1}^{n} (x - \hat{x})_i^2}{n}} \tag{9}$$

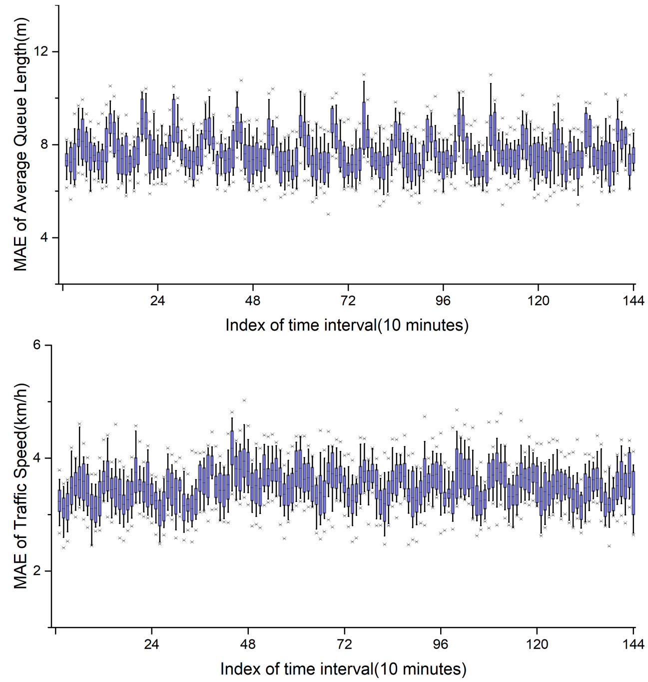

Fig. 12. Distribution of prediction error in time intervals.

$$MAE = \frac{1}{n}\sum_{i=1}^{n} |x_i - \hat{x}_i| \tag{10}$$

$$score = \frac{N_{(L=\hat{L})}}{N} \tag{11}$$

where n denotes the count of the predictions, x and $\hat{x}$ denote the prediction value and the truth value, respectively, and L and $\hat{L}$ denote the predicted value and the true value of the traffic state, respectively.

The accuracy statistics of the prediction are shown in Table IV and Fig. 11, and the MAE distribution of every time interval during the whole day is shown in Fig. 12.

According to the above statistics, the accuracy of the ST-RGAN method is comprehensively higher than that of the baseline methods for short-term predictions (within 30 minutes):

(1) Compared with the ST-RGCN method the accuracy of the traffic flow speed, average queue length, and traffic status

TABLE IV
EVALUATION OF THE RMSE AND MAE OF DIFFERENT MODELS

Parameter	Model	10 min		20 min		30 min		60 min	
		RMSE	MAE	RMSE	MAE	RMSE	MAE	RMSE	MAE
Traffic Flow Speed	SVR	5.29	4.16	5.85	4.55	6.42	4.94	7.62	5.78
	LSTM	4.53	3.57	4.62	3.64	4.78	3.76	6.00	4.54
	T-GCN	4.64	3.66	4.74	3.73	5.05	3.97	5.76	4.46
	ST-GCN	4.57	3.60	4.65	3.66	4.86	3.81	**5.64**	4.33
	ST-RGCN (ours)	4.50	3.54	4.60	3.61	4.75	3.72	5.77	4.38
	ST-RGAN (ours)	**4.44**	**3.48**	**4.54**	**3.56**	**4.66**	**3.65**	5.70	**4.31**
Average Queue Length	SVR	12.67	9.90	15.40	11.87	17.99	13.69	22.40	17.01
	LSTM	10.90	7.76	10.50	8.17	11.64	8.98	18.31	13.25
	T-GCN	11.19	8.68	12.57	9.76	13.63	10.54	17.62	13.37
	ST-GCN	10.32	7.96	11.46	8.86	12.62	9.72	**16.30**	**12.30**
	ST-RGCN (ours)	10.06	7.72	10.60	8.22	11.76	9.05	17.89	13.04
	ST-RGAN (ours)	**9.97**	**7.68**	**10.41**	**8.08**	**11.53**	**8.89**	17.30	12.65

is improved by 1.5%, 2.1%, and 0.2%, respectively, proving that the GAT is superior to the GCN in graph-structured data learning.

(2) Compared with the T-GCN and ST-GCN methods, the accuracy of the traffic flow speed, average queue length, and traffic status is improved by 2.2%-4.6%, 3.4%-11.1%, and 0.9%-1.7%, respectively, showing that the ST-Block and the structure in ST-RGAN can achieve better results in modelling the spatio-temporal pattern of the traffic.

(3) Compared with the SVR and LSTM methods, the accuracy of the traffic flow speed, average queue length, and traffic status is improved by 3.3%-28.5%, 3.1%-23.0%, and 0.9%-5.5%, showing that the introduction of a spatial dependencies can effectively improve the accuracy of a traffic prediction.

(4) Despite some fluctuations, the MAE values of the prediction parameters are still on the same horizontal line, showing that the prediction performance is relatively stable during the rush hours.

Similarly, for the prediction of the future 60 minutes, the ST-RGAN also shows superiority.

C. Analysis and Discussion

1) Accuracy of Average Queue Length Detection: As the analysis in Section II indicates, the sampling frequency of trace data influences the accuracy of traffic detection, especially the average queue length detection. Therefore, the accuracy of our method requires careful discussion.

Given the difficulty of obtaining the ground truth of the traffic parameter that is consistent with the trace data, a simulated analysis is adopted by implementing the transportation simulation software VISSIM [54].

In the simulation, the traffic of a one signal-intersection is simulated, and the floating-car position and the real-time queue length is output by the software every second. Then, the floating-car trace data are resampled to 10, 20, 30, 40, 50, and 60 s as the input to detect the average queue length of each aggregation interval of 1, 5 and 10 minutes. Finally, the accuracy of the detected average queue length is evaluated by comparing it with the average value output from the software.

The MAE of the average queue length under different sampling intervals and aggregation intervals is counted and is shown in Fig. 13, and the results taking the sampling point P_e as the queue start point are adopted for comparison.

As shown in Fig. 13, 1) the accuracy of the average queue length is significantly enhanced by using our method, especially for the low-frequency trace data; 2) a larger aggregation interval achieves a lower MAE, which proves that the fluctuation influenced by traffic lights has been weakened; 3) the MAE of the average queue length by using the proposed method is within 9.87 metres of the sampling interval from 10 s to 60 s under an aggregation interval of 10 minutes; and 4) the few floating cars within 1 minute lead to an unstable accuracy of traffic detection regardless of the sampling frequency.

2) Robustness of Traffic Prediction With ST-RGAN: Due to the inevitable noise during the data collection and traffic flow detection process, the prediction accuracy will be affected by the noise [25]. To test the robustness of the ST-RGAN model, random noise is introduced with the model inputs that are under 1%, 5%, 10%, 15%, and 20% of the input value, and the accuracy of prediction at different error levels is analysed.

Fig. 14 Accuracy of prediction with random errorshows the MAE of prediction results under different error levels of the input data. As shown by the results, the accuracy of the traffic speed prediction decreases 3.03% and 9.06% under input error levels of 10% and 20%, respectively, while the accuracy of the average queue length prediction decreases 8.67% and 19.8%, respectively. The results indicate that the

This article has been accepted for inclusion in a future issue of this journal. Content is final as presented, with the exception of pagination.

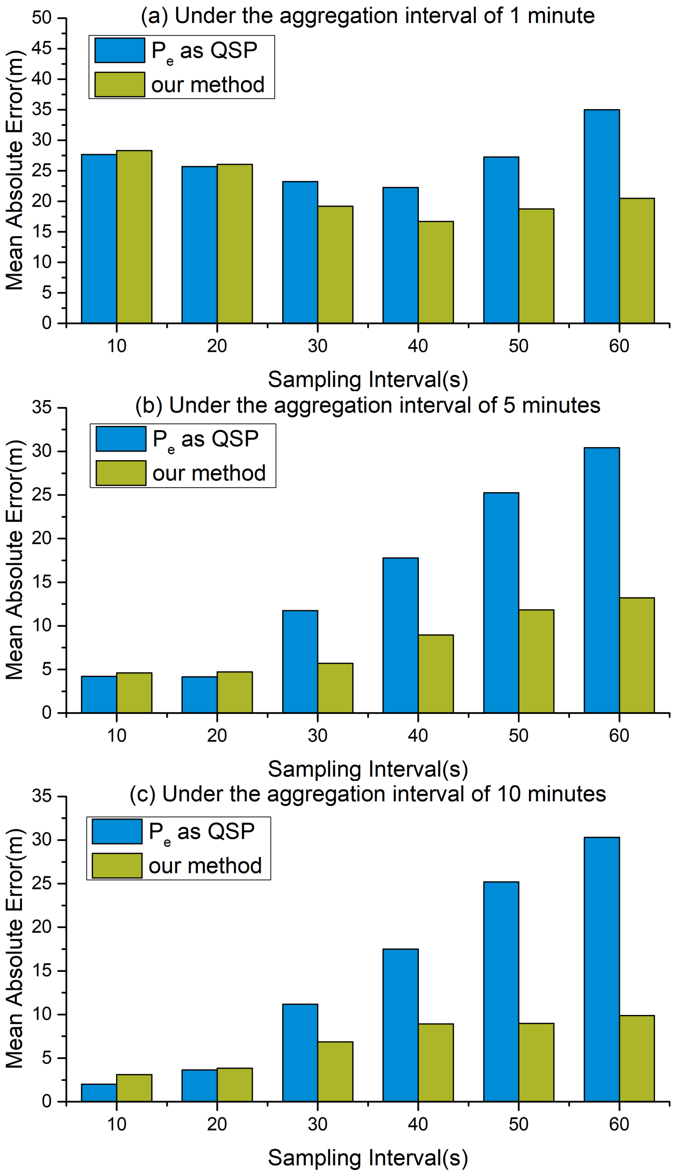

Fig. 13. Accuracy of average queue length detection under different trace sampling intervals and aggregation intervals.

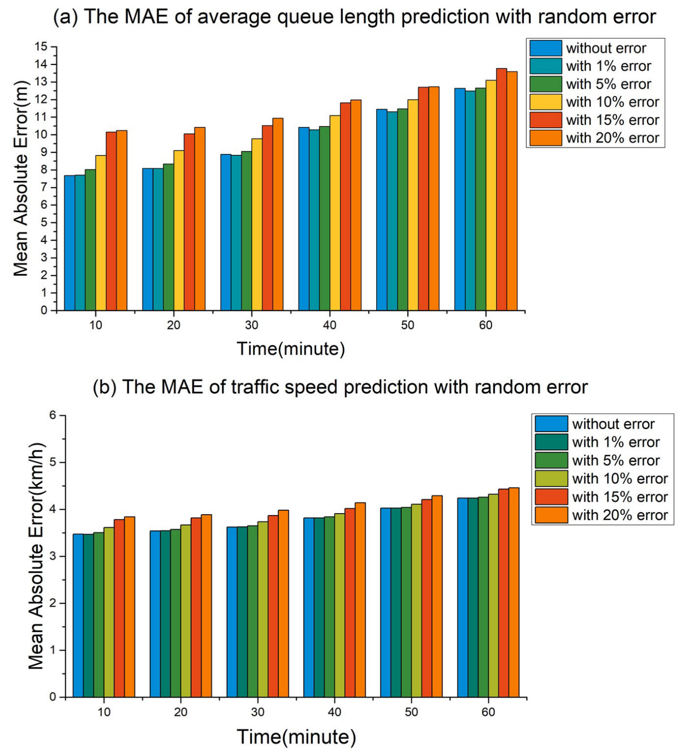

Fig. 14. Accuracy of prediction with random error.

TABLE V
CORRELATION COEFFICIENT OF SPATIAL FACTORS

	MAE of Traffic Flow Speed		MAE of Average Queue Length	
	coefficient	p	coefficient	p
Number of linked turns	0.19	0.10	-0.16	0.18
Traffic parameters` STD of linked turns	0.10	0.42	0.00	1.00
Traffic prediction`s MAE of linked turns	0.23	**0.05**	0.27	**0.02**

ST-RGAN has certain reliability and robustness, especially for traffic speed prediction.

3) Analysis of the Influencing Factors of Accuracy: To evaluate the factors affecting the prediction accuracy, Pearson correlation analysis and significance tests are performed to analyse the relationship between the accuracy and the attributes in the turn graph (such as the number of turns of one turn linked, the standard deviation of traffic parameters of linked turns, and the prediction error of linked turns). The result is shown in Table V.

According to the correlation coefficient and p-value, the findings are as follows.

(1) There is no significant correlation between the prediction accuracy and the number, the traffic parameters‘ standard deviation of linked turns, indicating that the prediction performance is relatively stable regardless of the node spatial attribute, even if the regional traffic is in a state of complex change.

(2) There is a significant positive correlation (p-value$<=$0.05) between the prediction accuracy of one turn and its linked turns, indicating that the errors influence each other between the upstream and downstream intersections.

V. CONCLUSION

To achieve turn-level traffic prediction with higher accuracy using big trace data, this research proposed a fine-grained traffic prediction method, named FTPG, which consists of two parts, namely, fine-grained traffic detection and short-term traffic prediction. In the former part, a novel method for estimation of the queue starting point is proposed to improve the accuracy of traffic information detection. In the latter part, aiming to capture the spatial dependency between traffic information, the topology is constructed at the turn level, and a GAT-based method, ST-RGAN, is proposed to improve the prediction accuracy. Experiments are performed using taxi

GPS trace data collected in the city of Wuhan, and the results show that the proposed FTPG method can obtain and predict traffic information (e.g., traffic flow speed, traffic state, and average queue length) accurately and reliably.

However, some improvements are still required to make the results of traffic predictions more accurate and credible. First, the external factors influencing the traffic conditions need to be considered and modelled, such as large public events, weather, holidays, and policy controls. Second, to capture the more complex traffic patterns, the adoption of more trace data with a longer time series is necessary to train and test the model. Finally, the accuracy of the prediction needs to be further evaluated using ground-truth data by measurement.

Acknowledgment

The authors would like to sincerely thank the anonymous reviewers for their constructive comments and valuable suggestions that improved the quality of this article.

References

[1] W. Alajali, W. Zhou, S. Wen, and Y. Wang, "Intersection traffic prediction using decision tree models," *Symmetry*, vol. 10, no. 9, p. 386, Sep. 2018, doi: 10.3390/sym10090386.

[2] Z. Kan, L. Tang, M.-P. Kwan, C. Ren, D. Liu, and Q. Li, "Traffic congestion analysis at the turn level using Taxis' GPS trajectory data," *Comput., Environ. Urban Syst.*, vol. 74, pp. 229–243, Mar. 2019, doi: 10.1016/j.compenvurbsys.2018.11.007.

[3] X. Kong, Z. Xu, G. Shen, J. Wang, Q. Yang, and B. Zhang, "Urban traffic congestion estimation and prediction based on floating car trajectory data," *Future Gener. Comput. Syst.*, vol. 61, pp. 97–107, Aug. 2016, doi: 10.1016/j.future.2015.11.013.

[4] Y. Sun, X. Yu, R. Bie, and H. Song, "Discovering time-dependent shortest path on traffic graph for drivers towards green driving," *J. Netw. Comput. Appl.*, vol. 83, pp. 204–212, Apr. 2017, doi: 10.1016/j.jnca.2015.10.018.

[5] A. Thakur and R. Malekian, "Fog computing for detecting vehicular congestion, an Internet of vehicles based approach: A review," *IEEE Intell. Transp. Syst. Mag.*, vol. 11, no. 2, pp. 8–16, Mar. 2019, doi: 10.1109/MITS.2019.2903551.

[6] X. Qian, T. Lei, J. Xue, Z. Lei, and S. V. Ukkusuri, "Impact of transportation network companies on urban congestion: Evidence from large-scale trajectory data," *Sustain. Cities Soc.*, vol. 55, Apr. 2020, Art. no. 102053, doi: 10.1016/j.scs.2020.102053.

[7] E. I. Vlahogianni, M. G. Karlaftis, and J. C. Golias, "Short-term traffic forecasting: Where we are and where we're going," *Transp. Res. C, Emerg. Technol.*, vol. 43, pp. 3–19, Jun. 2014, doi: 10.1016/J.TRC.2014.01.005.

[8] Y. Gu, W. Lu, L. Qin, M. Li, and Z. Shao, "Short-term prediction of lane-level traffic speeds: A fusion deep learning model," *Transp. Res. C, Emerg. Technol.*, vol. 106, pp. 1–16, Sep. 2019, doi: 10.1016/j.trc.2019.07.003.

[9] J. Zhang, Y. Zheng, D. Qi, R. Li, X. Yi, and T. Li, "Predicting citywide crowd flows using deep spatio-temporal residual networks," *Artif. Intell.*, vol. 259, pp. 147–166, Jun. 2018, doi: 10.1016/j.artint.2018.03.002.

[10] G. Hiribarren and J. C. Herrera, "Real time traffic states estimation on arterials based on trajectory data," *Transp. Res. B, Methodol.*, vol. 69, pp. 19–30, Nov. 2014, doi: 10.1016/j.trb.2014.07.003.

[11] A. Hofleitner, R. Herring, and A. Bayen, "Arterial travel time forecast with streaming data: A hybrid approach of flow modeling and machine learning," *Transp. Res. B, Methodol.*, vol. 46, no. 9, pp. 1097–1122, Nov. 2012, doi: 10.1016/j.trb.2012.03.006.

[12] X. Liu, F. Lu, H. Zhang, and P. Qiu, "Intersection delay estimation from floating car data via principal curves: A case study on Beijing's road network," *Frontiers Earth Sci.*, vol. 7, no. 2, pp. 206–216, Jun. 2013, doi: 10.1007/s11707-012-0350-y.

[13] P.-J. Tseng, C.-C. Hung, T.-H. Chang, and Y.-H. Chuang, "Real-time urban traffic sensing with GPS equipped probe vehicles," in *Proc. 12th Int. Conf. ITS Telecommun.*, Nov. 2012, pp. 306–310.

[14] L. Tang, Z. Kan, X. Zhang, X. Yang, F. Huang, and Q. Li, "Travel time estimation at intersections based on low-frequency spatial-temporal GPS trajectory big data," *Cartography Geograph. Inf. Sci.*, vol. 43, no. 5, pp. 417–426, Oct. 2016, doi: 10.1080/15230406.2015.1130649.

[15] M. Cetin, "Estimating queue dynamics at signalized intersections from probe vehicle data," *Transp. Res. Rec., J. Transp. Res. Board*, vol. 2315, no. 1, pp. 164–172, Jan. 2012, doi: 10.3141/2315-17.

[16] Z. Liang, H. Chen, Z. Song, Y. Zhou, and B. Zhang, "Traffic congestion incident detection and dissipation algorithm for urban intersection based on FCD," in *Proc. 3rd IEEE Int. Conf. Comput. Commun. (ICCC)*, Chengdu, China, Dec. 2017, pp. 2578–2583.

[17] Z. Yong-chuan, Z. Xiao-qing, Z. li-ting, and C. Zhen-ting, "Traffic congestion detection based on GPS floating-car data," *Procedia Eng.*, vol. 15, pp. 5541–5546, Dec. 2011, doi: 10.1016/j.proeng.2011.08.1028.

[18] F. Kong, J. Li, B. Jiang, and H. Song, "Short-term traffic flow prediction in smart multimedia system for Internet of vehicles based on deep belief network," *Future Gener. Comput. Syst.*, vol. 93, pp. 460–472, Apr. 2019, doi: 10.1016/j.future.2018.10.052.

[19] D. Srinivasan, C. Wai Chan, and P. G. Balaji, "Computational intelligence-based congestion prediction for a dynamic urban street network," *Neurocomputing*, vol. 72, nos. 10–12, pp. 2710–2716, Jun. 2009, doi: 10.1016/j.neucom.2009.01.005.

[20] S. Sun, C. Zhang, and G. Yu, "A Bayesian network approach to traffic flow forecasting," *IEEE Trans. Intell. Transp. Syst.*, vol. 7, no. 1, pp. 124–132, Mar. 2006, doi: 10.1109/TITS.2006.869623.

[21] X. Zhan, R. Li, and S. V. Ukkusuri, "Link-based traffic state estimation and prediction for arterial networks using license-plate recognition data," *Transp. Res. C, Emerg. Technol.*, vol. 117, Aug. 2020, Art. no. 102660, doi: 10.1016/j.trc.2020.102660.

[22] C. Zhang, J. J. Q. Yu, and Y. Liu, "Spatial-temporal graph attention networks: A deep learning approach for traffic forecasting," *IEEE Access*, vol. 7, pp. 166246–166256, 2019, doi: 10.1109/ACCESS.2019.2953888.

[23] Y. Zhang, T. Cheng, and Y. Ren, "A graph deep learning method for short–term traffic forecasting on large road networks," *Comput.-Aided Civil Infrastruct. Eng.*, vol. 34, no. 10, pp. 877–896, Oct. 2019, doi: 10.1111/mice.12450.

[24] S. Guo, Y. Lin, N. Feng, C. Song, and H. Wan, "Attention based spatial-temporal graph convolutional networks for traffic flow forecasting," in *Proc. AAAI*, vol. 33, 2019, pp. 922–929, doi: 10.1609/aaai.v33i01.3301922.

[25] L. Zhao *et al.*, "T-GCN: A temporal graph ConvolutionalNetwork for traffic prediction," 2018, *arXiv:1811.05320*. [Online]. Available: http://arxiv.org/abs/1811.05320

[26] X. Yang, L. Tang, L. Niu, X. Zhang, and Q. Li, "Generating lane-based intersection maps from crowdsourcing big trace data," *Transp. Res. C, Emerg. Technol.*, vol. 89, pp. 168–187, Apr. 2018, doi: 10.1016/j.trc.2018.02.007.

[27] Y. Goda, L. Zhang, and S. Serikawa, "Proposal a vehicle speed measuring system using image processing," in *Proc. Int. Symp. Comput., Consum. Control*, Taichung, Taiwan, Jun. 2014, pp. 541–543.

[28] B. Coifman, "Identifying the onset of congestion rapidly with existing traffic detectors," *Transp. Res. A, Policy Pract.*, vol. 37, no. 3, pp. 277–291, 2003, doi: 10.1016/S0965-8564(02)00016-2.

[29] M. R. Friesen and R. D. McLeod, "Bluetooth in intelligent transportation systems: A survey," *Int. J. Intell. Transp. Syst. Res.*, vol. 13, no. 3, pp. 143–153, Sep. 2015, doi: 10.1007/s13177-014-0092-1.

[30] Y. Sun, H. Song, A. J. Jara, and R. Bie, "Internet of Things and big data analytics for smart and connected communities," *IEEE Access*, vol. 4, pp. 766–773, 2016, doi: 10.1109/ACCESS.2016.2529723.

[31] J. Zheng and H. X. Liu, "Estimating traffic volumes for signalized intersections using connected vehicle data," *Transp. Res. C, Emerg. Technol.*, vol. 79, pp. 347–362, Jun. 2017, doi: 10.1016/j.trc.2017.03.007.

[32] G. Comert and M. Cetin, "Queue length estimation from probe vehicle location and the impacts of sample size," *Eur. J. Oper. Res.*, vol. 197, no. 1, pp. 196–202, Aug. 2009, doi: 10.1016/j.ejor.2008.06.024.

[33] L. Tisljaric, T. Erdelic, and T. Caric, "Analysis of intersection queue lengths and level of service using GPS data," in *Proc. Int. Symp.*, Zadar, Croatia, Sep. 2018, pp. 43–46.

[34] F. Wen, G. Zhang, L. Sun, X. Wang, and X. Xu, "A hybrid temporal association rules mining method for traffic congestion prediction," *Comput. Ind. Eng.*, vol. 130, pp. 779–787, Apr. 2019, doi: 10.1016/j.cie.2019.03.020.

[35] X. Ma, Z. Dai, Z. He, J. Ma, Y. Wang, and Y. Wang, "Learning traffic as images: A deep convolutional neural network for large-scale transportation network speed prediction," *Sensors*, vol. 17, no. 4, p. 818, Apr. 2017, doi: 10.3390/s17040818.

[36] Y. Shu, “Wireless traffic modeling and prediction using seasonal ARIMA models,” *IEICE Trans. Commun.*, vols. E88-B, no. 10, pp. 3992–3999, Oct. 2005, doi: 10.1093/ietcom/e88-b.10.3992.

[37] T. Thomas, W. Weijermars, and E. van Berkum, “Predictions of urban volumes in single time series,” *IEEE Trans. Intell. Transp. Syst.*, vol. 11, no. 1, pp. 71–80, Mar. 2010, doi: 10.1109/TITS.2009.2028149.

[38] D. Satrinia and G. A. P. Saptawati, “Traffic speed prediction from GPS data of taxi trip using support vector regression,” in *Proc. Int. Conf. Data Softw. Eng. (ICoDSE)*, South Sumatera, Indonesia, Nov. 2017, pp. 1–6.

[39] F. Kong, J. Li, B. Jiang, T. Zhang, and H. Song, “Big data-driven machine learning-enabled traffic flow prediction,” *Trans. Emerg. Telecommun. Technol.*, vol. 30, no. 9, Sep. 2019, doi: 10.1002/ett.3482.

[40] Y. Wu, H. Tan, L. Qin, B. Ran, and Z. Jiang, “A hybrid deep learning based traffic flow prediction method and its understanding,” *Transp. Res. C, Emerg. Technol.*, vol. 90, pp. 166–180, May 2018, doi: 10.1016/J.TRC.2018.03.001.

[41] B. Yu, H. Yin, and Z. Zhu, “Spatio-temporal graph convolutional networks: A deep learning framework for traffic forecasting,” in *Proc. 27th Int. Joint Conf. Artif. Intell.*, Stockholm, Sweden, Jul. 2018, pp. 3634–3640.

[42] M. M. Chowdhury, M. Hasan, S. Safait, D. Chaki, and J. Uddin, “A traffic congestion forecasting model using CMTF and machine learning,” in *Proc. Joint 7th Int. Conf. Informat., Electron. Vis. (ICIEV)*, Jun. 2018, pp. 357–362.

[43] B. Li, W. Cheng, and L. Li, “Real-time prediction of lane-based queue lengths for signalized intersections,” *J. Adv. Transp.*, vol. 2018, pp. 1–18, Dec. 2018, doi: 10.1155/2018/5020518.

[44] B. Li, Z. Yu, L. Huang, and B. Guo, “Vehicle departure pattern and queue length prediction at an isolated intersection with automatic vehicle identity detection,” *IET Intell. Transp. Syst.*, vol. 13, no. 12, pp. 1804–1813, Dec. 2019, doi: 10.1049/iet-its.2019.0117.

[45] B. Y. Chen, H. Yuan, Q. Li, W. H. K. Lam, S.-L. Shaw, and K. Yan, “Map-matching algorithm for large-scale low-frequency floating car data,” *Int. J. Geograph. Inf. Sci.*, vol. 28, no. 1, pp. 22–38, Jan. 2014, doi: 10.1080/13658816.2013.816427.

[46] L. Tang, C. Ren, Z. Liu, and Q. Li, “A road map refinement method using delaunay triangulation for big trace data,” *ISPRS Int. J. Geo-Inf.*, vol. 6, no. 2, p. 45, Feb. 2017, doi: 10.3390/ijgi6020045.

[47] I. El-Shawarby, H. Rakha, V. W. Inman, and G. W. Davis, “Evaluation of driver deceleration behavior at signalized intersections,” *Transp. Res. Rec., J. Transp. Res. Board*, vol. 2018, no. 1, pp. 29–35, Jan. 2007, doi: 10.3141/2018-05.

[48] J. F. Yu, L. Wang, and X. L. Gong, “Classification research based on the congestion of urban intersection,” *Appl. Mech. Mater.*, vols. 209–211, pp. 759–762, Oct. 2012, doi: 10.4028/www.scientific.net/AMM.209-211.759.

[49] M.-B. Hu, R. Jiang, Y.-H. Wu, W.-X. Wang, and Q.-S. Wu, “Urban traffic from the perspective of dual graph,” *Eur. Phys. J. B*, vol. 63, no. 1, pp. 127–133, May 2008, doi: 10.1140/epjb/e2008-00219-5.

[50] S. Hochreiter and J. Schmidhuber, “Long short-term memory,” *Neural Comput.*, vol. 9, no. 8, pp. 1735–1780, Nov. 1997, doi: 10.1162/neco.1997.9.8.1735.

[51] P. Velickovic, G. Cucurull, A. Casanova, A. Romero, P. Liò, and Y. Bengio, “Graph Attention Networks,” 2017, *arXiv:1710.10903*. [Online]. Available: https://arxiv.org/abs/1710.10903

[52] T. Wu, F. Chen, and Y. Wan, “Graph attention LSTM network: A new model for traffic flow forecasting,” in *Proc. 5th Int. Conf. Inf. Sci. Control Eng. (ICISCE)*, Zhengzhou, China, Jul. 2018, pp. 241–245.

[53] A. Vaswani *et al.*, “Attention is all you need,” 2017, *arXiv:1706.03762*. [Online]. Available: http://arxiv.org/abs/1706.03762

[54] M. Fellendorf and P. Vortisch, “Microscopic traffic flow simulator VISSIM,” in *Fundamentals of Traffic Simulation* (International Series in Operations Research & Management Science), vol. 145, J. Barceló, Ed. New York, NY, USA: Springer, 2010, pp. 63–93, doi: 10.1007/978-1-4419-6142-6_2.

Mengyuan Fang (Graduate Student Member, IEEE) received the M.E. degree from Wuhan University, Wuhan, China, in 2020, where he is currently pursuing the Ph.D. degree with the State Key Laboratory of Information Engineering in Surveying, Mapping, and Remote Sensing. His research interests include spatio-temporal data mining and intelligent transportation systems. He is a Student Member of CCF.

Luliang Tang received the Ph.D. degree from Wuhan University, Wuhan, China, in 2007. He is currently a Professor with Wuhan University. His research interests include space–time GIS, deep learning, GIS for transportation, and change detection.

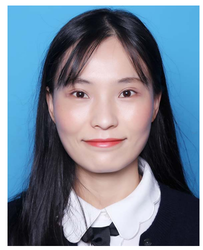

Xue Yang received the Ph.D. degree from Wuhan University, Wuhan, China, in 2018. She is currently an Assistant Professor with the China University of Geosciences, Wuhan, China. Her research interests include intelligent transportation systems, spatiotemporal data analysis, and information mining.

Yang Chen received the M.E. degree from Liaoning Technical University, Fuxin, China, in 2019. He is currently pursuing the Ph.D. degree with the State Key Laboratory of Information Engineering in Surveying, Mapping, and Remote Sensing, Wuhan University, Wuhan, China. He was a jointly educates student with the China Academy of Surveying and Mapping, Beijing, China, from 2017 to 2019. His research interests include deep learning and intelligent remote sensing information processing.

Chaokui Li received the Ph.D. degree from Central South University, Changsha, China, in 2001. He is currently a Professor with the Hunan University of Science and Technology. His research interests include 3D geographic modeling and geographic information systems.

Qingquan Li received the Ph.D. degree in geographic information system (GIS) and photogrammetry from the Wuhan Technical University of Surveying and Mapping, Wuhan, China, in 1998. He is currently a Professor with Shenzhen University, Guangdong, China, and Wuhan University, Wuhan. His research interests include dynamic data modeling in GIS, surveying engineering, and intelligent transportation systems.